



# HHS Public Access

Author manuscript

*J Aerosol Sci.* Author manuscript; available in PMC 2015 December 11.

Published in final edited form as:

*J Aerosol Sci.* 2012 May ; 47: 100–110. doi:10.1016/j.jaerosci.2012.01.002.

## Comparison of diffusion charging and mobility-based methods for measurement of aerosol agglomerate surface area

Bon Ki Ku\* and Pramod Kulkarni

Centers for Disease Control and Prevention (CDC), National Institute for Occupational Safety and Health (NIOSH), 4676 Columbia Parkway, MS-R3, Cincinnati, Ohio 45226, USA

### Abstract

We compare different approaches to measure surface area of aerosol agglomerates. The objective was to compare field methods, such as mobility and diffusion charging based approaches, with laboratory approach, such as Brunauer, Emmett, Teller (BET) method used for bulk powder samples. To allow intercomparison of various surface area measurements, we defined ‘geometric surface area’ of agglomerates (assuming agglomerates are made up of ideal spheres), and compared various surface area measurements to the geometric surface area. Four different approaches for measuring surface area of agglomerate particles in the size range of 60–350 nm were compared using (i) diffusion charging-based sensors from three different manufacturers, (ii) mobility diameter of an agglomerate, (iii) mobility diameter of an agglomerate assuming a linear chain morphology with uniform primary particle size, and (iv) surface area estimation based on tandem mobility–mass measurement and microscopy. Our results indicate that the tandem mobility–mass measurement, which can be applied directly to airborne particles unlike the BET method, agrees well with the BET method. It was also shown that the three diffusion charging-based surface area measurements of silver agglomerates were similar within a factor of 2 and were lower than those obtained from the tandem mobility–mass and microscopy method by a factor of 3–10 in the size range studied. Surface area estimated using the mobility diameter depended on the structure or morphology of the agglomerate with significant underestimation at high fractal dimensions approaching 3.

### Keywords

Diffusion charging; Aerosol surface area; Agglomerates; Tandem mobility–mass approach; Mobility diameter; BET method

## 1. Introduction

The impetus for measuring surface area of aerosols in ambient and work environments comes from recent toxicological studies which have shown that the surface area of ultrafine

---

\*Corresponding author: Tel.: +1 513 841 4147; fax: +1 513 841 4545. BKu@cdc.gov (B.K. Ku).

### Disclaimer

The mention of any company or product does not constitute an endorsement by the Centers for Disease Control and Prevention. The findings and conclusions in this paper are those of the authors and do not necessarily represent the views of the National Institute for Occupational Safety and Health.

and nanoparticles correlates better with the biological response than their mass (LeBlanc et al., 2010; Nurkiewicz et al., 2009; Singh et al., 2007; Oberdörster et al., 2005; Nel et al., 2006; Stoeger et al., 2006; Sager & Castranova, 2009). These studies have exclusively used the Brunauer, Emmett, Teller (BET) surface area as a metric in their animal studies, prompting recommendations to use surface area as an exposure metric. As a result, many studies (Elihn and Berg, 2009; Brouwer et al., 2009; Evans et al., 2010; Park et al., 2009; Bau et al., 2011; LeBouf et al., 2011) have used various approaches, including diffusion chargers (DCs), to measure “surface area” as a surrogate measure of BET surface area. The instrument designed specifically to measure aerosol surface area was the epiphaniometer (Gäggeler et al., 1989). This device, which is now discontinued as a commercial product, measures active surface area of the aerosol by measuring the attachment rate of radioactive lead atoms to aerosol particles; however, it is not well suited for routine field use because of the inclusion of a radioactive source. Current available methods for measuring particle surface area include diffusion charging-based sensors (DCS), mobility analysis, transmission electron microscopy (TEM), and the Brunauer, Emmett, Teller (BET) method for bulk powder samples. While the BET method, a laboratory method, is used to measure BET surface area for bulk powder samples as a metric in toxicology studies, methods for measuring surface area of airborne particles unlike the BET method are not readily available. A diffusion charging-based sensor (DCS) has an advantage of portability and real time capability, but its limitation is that it does not provide a direct measure of surface area, much like a photometer or nephelometer used for particle mass measurement. Many real-world aerosols are agglomerates (particularly in work environments) and are far from ideal aerosols used in the calibration of DCS. DC instruments have been increasingly used in field studies involving real-world agglomerates (Elihn and Berg, 2009; Buonanno et al., 2010; Evans et al., 2010; Brouwer et al., 2009; Ntziachristos et al., 2007). Many studies do not acknowledge that the DC surface area in itself is a different metric, and is not same as the BET surface area, and use DC beyond the applicable particle size ranges. A recent study showed that the active particle surface area measured by the diffusion charging based sensor is comparable to the geometric surface area (as measured by TEM) for silver agglomerates below 100 nm, but in the size range over 100 nm, it underestimates the geometric surface area (Ku & Maynard, 2005). A related study showed that the DCS-measured surface area deviates significantly from the geometric surface area as the particle size increases up to 900 nm for spherical particles (Ku, 2009, 2010).

The purpose of this study was to assess the difference of mobility and DCS methods, which are simple and most practical methods to use from exposure monitoring point of view, from more rigorous methods such as the BET method for measurement of agglomerate surface area. To allow intercomparison of various surface area measurements, we defined ‘geometric surface area’ of agglomerates (assuming agglomerates are made up of ideal spheres), and compared various surface area measurements to the geometric surface area. Four approaches for measuring the surface area of agglomerate aerosols in the submicrometer size range were compared:

1. An approach involving the tandem measurement of agglomerate mobility and mass using differential mobility analyzer and aerosol particle mass analyzer (APM),

followed by primary particle size measurement using the transmission electron microscopy (TEM) to estimate the surface area.

2. The diffusion charging approach, using three different commercially available diffusion charging-based sensors.
3. Measurement of the surface area based directly on mobility diameter assuming spherical particles.
4. Surface area measurement based on mobility diameter with correction to account for primary particle size.

These approaches were evaluated using agglomerated aerosols of known properties. An intercomparison of these methods is presented, and the results are discussed.

## 2. Experimental

### 2.1. Approaches used for measurement of surface area

The first approach (referred to as APM–TEM) for measurement of surface area of agglomerates involved measurement of particle mass of mobility classified particles using aerosol particle mass analyzer (APM) and primary particle size using transmission electron microscopy (TEM). If an agglomerate consists of many primary particles with an approximately uniform primary particle diameter, and if mass of the agglomerate ( $M$ ) and the primary particle size are known ( $d_p$ ), surface area of the agglomerate ( $A_t$ ) can be calculated using the following equation:

$$\frac{A_t}{M} = \frac{6}{\rho d_p} \quad (1)$$

where  $\rho$  is the density of the primary particle. This equation assumes all primary particles have the same size, and no necking between primary particles. In this study, we estimated the average mass of monodisperse agglomerate particles using an aerosol particle mass analyzer (APM-3600, Kanomax). The APM utilizes two coaxial cylindrical electrodes rotating at the same speed. Charged particles enter the annular gap rotating at the same speed (the APM rotating speed was 3000 rpm for all measurements except for PSL 60 nm when it was 5000 rpm in this study) as the electrodes. As a voltage is applied to the inner electrode, the particles experience directly opposing centrifugal and electrostatic force. These forces are in balance for particles of a specific mass-to-charge ratio, allowing the particles to traverse through the APM (Ehara et al., 1996; Ku et al., 2006). Primary particle size  $d_p$  was obtained by analyzing about 100–150 particles using the transmission electron microscopy. The density of the particle was assumed to be same as the bulk density of the material. Using the values of  $M$ ,  $\rho$ , and  $d_p$  values of  $A_t$  were estimated using the above equation.

The second approach (referred to as DCS) consisted of estimation of surface area using the diffusion charging-based sensors. The measurement scheme in diffusion charging-based sensors involves the use of attachment of unipolar ions to particles by diffusion followed by detection of particle current. Ions undergoing Brownian motion attach to particle surface,

imparting an electrical charge to the particles (Dhaniyala et al., 2011). Subsequently, the charged particles are trapped on a particle filter where the total charge of the particles is measured by an aerosol electrometer, which is related to particle surface area as follows (Matter Engineering AG, 2001):

$$A_{DCS} = \frac{1}{e \sqrt{3kT/m_{ion}nN}} I \quad (2)$$

where  $I$  is current of the charged particles,  $m_{ion}$  is the ion mass,  $n$  is the ion concentration,  $N$  is the particle concentration,  $k$  is the Boltzmann constant,  $T$  is the absolute temperature of the surrounding gas, and  $e$  is the elementary charge. Eq. (2) is a general equation that gives active surface area and is applicable to all diffusion chargers that satisfy the implicit assumptions. It is worth noting that due to charge build-up on the particles, the DC sensor response may be different from the Epiphaniometer response. Eq. (2) represents the surface area per agglomerate particle.

Three commercially available diffusion charging sensors were used in this study to compare their responses: DC2000CE (Ecochem, USA), LQ1-DC (Matter Engineering, Switzerland; this is discontinued as a commercial product), and the Nanoparticle Surface Area Monitor (NSAM; Model 3550, TSI Inc.). These are semi-empirical instruments that give a size-integrated response proportional to input surface area. The first two sensors measure the so-called “active surface area” of the aerosol directly (Keller et al., 2001), whereas the NSAM measures the lung-deposited surface area of the aerosol (consistent with ICRP curve; Fissan et al., 2007). Active surface area is defined as the surface of a particle that is involved in interactions with the surrounding gas (Keller et al., 2001) and lung deposited surface area defined as the surface of a particle deposited in the alveolar or tracheobronchial region with its deposition efficiency based on the ICRP curve (Fissan et al., 2007). To facilitate comparison of response of all three sensors using a common metric, the NSAM measurements were inverted back to active surface area using a diameter-dependent deposition efficiency obtained from the ICRP (1994) curve.

For conversion of the NSAM data to surface area provided to the inlet of NSAM, once the data from the NSAM were obtained for each single mobility diameter, a fraction of lung-deposition (alveolar deposition) for each particle size was first found based on the ICRP curve and then, the NSAM data were divided by the deposition fraction for each diameter to give surface area comparable to the other DCs data. The related equation can be expressed:

$$S_{LD} = f(d_m) \cdot S_{NSAM}^{IN} \quad (3)$$

where  $S_{LD}$  is a value on the monitor of NSAM (which is called a lung-deposited surface area),  $f(d_m)$  is a fraction of particles deposited in the alveolar region at mobility diameter of  $d_m$ , and  $S_{NSAM}^{IN}$  is surface area at the inlet of NSAM.  $f(d_m)$  is expressed as follows (Hinds, 1999):

$$f(d_m) = \left( \frac{0.0155}{d_m} \right) \left[ \exp(-0.416(\ln(d_m) + 2.84)^2) + 19.11 \exp(-0.482(\ln(d_m) - 1.362)^2) \right] \quad (4)$$

where  $d_m$  is particle mobility size in  $\mu\text{m}$ .

The third approach (referred to as MD) was based on the estimation of surface area directly from the particle's mobility diameter ( $d_m$ ), assuming a spherical shape, and is given by

$$A_{MD} = \pi d_m^2 \quad (5)$$

The fourth approach (referred to as mobility diameter and linear chain approximation [MD-LCA]) was based on estimation of surface area using mobility diameter of the agglomerate, but assuming linear chain morphology instead of a spherical shape, as was done in the MD approach above. This simplifying assumption was introduced by Lall and Friedlander (2006) where the agglomerate with mobility diameter ( $d_m$ ) is assumed to be a linear chain of spherical particles, each with radius  $a$ , such that (Lall & Friedlander, 2006)

$$\frac{d_m}{C(d_m)} = \frac{c^* N_p a^2}{3\pi\lambda} \quad (6)$$

where  $N_p$  is number of primary particles in an agglomerate,  $C$  is the slip correction factor,  $c^*$  is the dimensionless drag force for agglomerates ( $c^* = 9.17$  for orientation-averaged motion, and  $c^* = 6.62$  for motion parallel to viscous flow of gas (Chan & Dahneke, 1981)), and  $\lambda$  is the mean free path of the gas. For agglomerates with a fractal dimension not greater than 2, the number of primary particles in an agglomerate with primary particle size in the free molecular regime can be calculated from Eq. (6). Therefore, the total surface area,  $A_{LCA}$ , of the agglomerate can be obtained by summing over all primary particles in the agglomerate, assuming no necking between primary particles:

$$A_{LCA} = N_p 4\pi a^2 \quad (7)$$

Because of the linear chain approximation, the above approach is suitable for agglomerates with fractal dimension close to 1. We used the standard MD-LCA correction module available in the TSI AIMS software. Table 1 summarizes the definition of different surface area from each instrument used in this study.

## 2.2. Experimental setup

Fig. 1 shows a schematic diagram of an experimental setup used for measuring aerosol surface area employing the approaches mentioned above. Three types of aerosol were generated. Silver agglomerates were generated by the evaporation/condensation generator using conditions described earlier (Ku & Maynard, 2006), and polystyrene latex (PSL, Duke Scientific Corp.) particles were generated using an electrospray generator (Ku & Kulkarni, 2009) that was modified to provide higher liquid flow rates with a larger capillary (100  $\mu\text{m}$  I.D.).  $\text{TiO}_2$  agglomerates were obtained by aerosolizing the  $\text{TiO}_2$  powder (P25, Evonik-Degussa) using a vortex shaker (Ku et al., 2006). To generate agglomerates of PSL particles, 20 nm PSL particles were first electrosprayed and then collected into a coagulation chamber ( $\sim 20$  L volume) for aging and subsequent classification using a differential mobility

analyzer (DMA; TSI Inc. Model 3081; with sheath air flow of 6–10 Lpm and aerosol flow of 1.0 Lpm). An impactor (0.0457 cm nozzle diameter, TSI Inc.) at the inlet of the DMA was used to remove particles larger than 1  $\mu\text{m}$  aerodynamic diameter. The DMA-classified aerosol fraction was passed through a neutralizer and a cylindrical electrostatic precipitator to provide uncharged monodisperse test particles.

### 3. Results and discussion

#### 3.1. Test aerosol characterization

Fig. 2 shows a log–log plot of mass versus mobility diameter for silver, PSL, and  $\text{TiO}_2$  agglomerates, with primary particle sizes of 18, 20, and 22.5 nm, respectively. A mass scaling factor ( $D_f$ ) was defined as  $M \propto (d_m)^{D_f}$  and was used in lieu of fractal dimension to account for the possibility that the particles may not exhibit characteristics of true fractals. In Fig. 2, the mass scaling factor  $D_f$  is equal to the slope of the linear fit. Silver agglomerates had a  $D_f$  of 2.0 while that for PSL agglomerates with primary particle diameters of 20 nm was 2.37, and for  $\text{TiO}_2$  agglomerates it was 2.63. This suggests a more open structure of silver agglomerates compared to  $\text{TiO}_2$  and PSL agglomerates.

#### 3.2. Surface area measurement using the APM–TEM method

Fig. 3a shows a typical number distribution, measured downstream of the APM, as a function of the APM classifying voltage for two different types of mobility-classified monodisperse aerosols. For each APM voltage, the particle number concentration was measured by the CPC (TSI 3022a), and the peak APM voltage corresponding to the peak mass for the mobility-selected particles was determined. We used this peak voltage to determine the “average” particle mass of DMA-classified agglomerate particles. The primary particle diameters of the silver and  $\text{TiO}_2$  agglomerates were measured using the TEM analysis. The distribution of primary particle diameters of silver agglomerates is shown in Fig. 3b; primary particles ranged from 8 to 32 nm in diameter with most of the particles having a diameter of 18 nm. The peak primary particle diameter of 18 nm was used for silver agglomerates in the subsequent analysis and closely agrees with earlier studies using a similar experimental setup (Lall et al., 2006; Kim et al., 2009). Distribution of primary particle diameters of  $\text{TiO}_2$  agglomerates ranged from 10 to 46 nm with a peak diameter of 22.5 nm (Fig. 3b). The primary particle diameter estimation of  $\text{TiO}_2$  agglomerates was more challenging due to significant necking and sintering of primary particle pairs. The primary particle diameter was estimated by taking the mean of the largest and smallest diameter encompassing a primary particle. Our estimate of peak diameter of 22.5 nm is slightly smaller than that reported by the manufacturer (25 nm based on Brunauer, Emmett, Teller [BET] analysis), and earlier studies (26–27 nm) (Braydich-Stolle et al., 2009; Suttiponparnit et al., 2011). The primary particle diameter of PSL agglomerate was assumed to be 20 nm on the basis of suspension made up of NIST traceable 20 nm PSL standard (Duke Scientific) that was used to electrospray the aerosol.

The accuracy and precision of surface area measurement by the APM–TEM method depends on many factors, such as (i) uncertainty in estimating primary particle size by TEM, (ii) measurement precision or width of transfer function of the APM, (iii) fluctuation in

aerosol concentration, and (iv) fraction of multiply charged particles passing through the APM. The last factor, the multiply charged fraction, can introduce large uncertainties in the measurement depending on the particle size distribution of the aerosol entering the APM. To probe the extent of combined effect of these sources of uncertainties, we compared the surface area measured by the APM–TEM method with that obtained from an independent method for TiO<sub>2</sub> and PSL aerosols. Surface area of TiO<sub>2</sub> was obtained using BET analysis, whereas for the PSL aerosol (consisting of only singlet monomers, not agglomerates), the surface area was estimated based on the precisely known diameter of the NIST-traceable PSL standard spheres. Fig. 3c shows this comparison of input surface area of TiO<sub>2</sub> and PSL aerosol with the surface area measured using APM–TEM analysis. Input surface area for TiO<sub>2</sub> agglomerates was calculated by multiplying the BET-measured “specific surface area” (SSA) of the bulk TiO<sub>2</sub> sample (100 mg) by the peak particle mass obtained from the APM assuming unit charge on the particles. Table 2 shows this estimated surface area for three diameters using the above approach. As seen in Fig. 3c, the surface area from the APM–TEM method shows good agreement with the input surface area, within 5.1% for the PSL particles and 15.0% for the TiO<sub>2</sub> agglomerates. It is worth noting that the BET surface area is derived from measurement on large mass of bulk sample on the order of few hundred milligrams, whereas the APM mass measured in our experiments is on the order of femtograms. The fact that the BET surface area agrees well with that from the APM–TEM method based on a much smaller mass suggests that the TiO<sub>2</sub> aerosol is quite homogeneous. For TiO<sub>2</sub> agglomerates, there is an excellent agreement at lower mobility diameters (<250 nm); however, at large mobility diameter (>350 nm) the APM–TEM approach tends to overestimate the surface area. This is possibly due to the peak location of the APM transfer function and multiply charged fraction of particles. The effect of the multiply charged particles classified by the DMA may be not as much on the peak location of the APM transfer function because APM measures mass/charge—multiply charged particles from the DMA have higher mass and with higher charge contribute approximately to a similar peak location, but with a broad mass distribution (assuming the multiply charged fraction is small). Barone et al. recently reported the combined DMA-APM transfer function and its possible effect on particle mass from the location of the peak in the APM (Barone et al., 2011). The increase of the location of the peak leads to overestimation of particle mass by the APM, and therefore overestimation of surface area. The deviation from input surface area at 350 nm was about 15.0%. Nevertheless, this demonstrates reasonable difference between the APM–TEM approach and BET surface area for it to be used as a benchmark method in this study.

### 3.3. Comparison of surface area measurements

#### 3.3.1. Surface area measurements from three DCSs and APM–TEM approach

—In this section DCS data are used to explain the differences between active and geometric surface area, and to clearly convey that these surface areas are different metrics and any comparison only serves to bring out the difference in methods themselves rather than quantifying their accuracy or error.

Fig. 4 shows surface areas measured by three diffusion charging-based sensors (DC2000CE, NSAM, and LQ1-DC) and that obtained from the APM–TEM approach for three different

particle agglomerates, i.e., silver, PSL, and TiO<sub>2</sub>. For comparison, the surface area on the y-axis was normalized by particle number concentration to give surface area per particle. The surface areas from the three diffusion charging-based sensors and the APM-TEM approach increase as the mobility diameter increases; the difference in surface area estimation between the two methods also gradually increases with increasing size. Compared to the APM-TEM method, the surface area from DCS is significantly underestimated, particularly for the larger agglomerates. The difference in response of various diffusion charging sensors is also significant. For silver agglomerates, the surface area from LQ1-DC is higher compared to that from the other two DCs (by a factor of ~2), while the measurements by DC2000CE and NSAM are similar.

The data in Fig. 4 show that for particles in the submicrometer size range, compared to APM-TEM approach, the three diffusion charging-based sensors significantly underestimate the surface area by a factor of 3–10. The DC2000CE, LQ1-DC, and NSAM underestimate the surface area by up to 96%, 92%, and 83%, respectively, in the particle size range of 100–300 nm. This result confirms previous data suggesting that the two diffusion charging-based sensors (DC2000CE and LQ1-DC) underestimated the surface area in the particle size range of 100–200 nm for agglomerate particles (Ku & Maynard 2005).

Also shown in Fig. 4 are measurements of surface area of spherical singlet particles of PSL using diffusion-charging sensors (LQ1-DC) from a recent study (Ku, 2010; shown by a dotted line) in the size range of 100–400 nm. The figure clearly shows that the underestimation of surface area from diffusion charging sensors is more drastic for agglomerates than for the spherical monomers. For example, for 300 nm particles, the surface area of spherical monomers was underestimated by 88% (Ku, 2010), while for the agglomerates of the same mobility size in this study, the surface area was underestimated by 92–96%. This indicates that the measurement difference is larger for agglomerates compared to spherical particles. This difference could be much higher for complex aerosols with high dynamic shape factor or large internal surface area, such as carbon nanotube agglomerates.

### 3.3.2. Surface area measurements from MD and MD-LCA and APM-TEM approach

—Fig. 5 shows comparison of measured surface areas from two mobility diameter-based approaches (MD and MD-LCA). The mobility diameter-based approaches are in reasonable agreement with the APM-TEM for silver agglomerates, while they underestimate the surface area for PSL and TiO<sub>2</sub> agglomerates. This difference is attributed to the difference in the structure of agglomerates as will be discussed later. As noted earlier for diffusion charging-based sensors, in case of both MD and MD-LCA approaches, the deviation from the APM-TEM method also increases with increasing mobility size of the agglomerate. TiO<sub>2</sub> agglomerates showed highest deviation compared to silver and PSL particles, though the error is much lower compared to that from the DCS measurements. Based on the analysis for two options of the TSI SMPS module for silver agglomerates (one is that agglomerate orientation in DMA is parallel to relative motion and the other is randomly oriented), the difference between APM-TEM and MD-LCA for the case of parallel alignment in the DMA are higher for agglomerates with sizes below 200 nm than those for random orientation while the opposite happens for agglomerates larger than 200

nm. It is hypothesized that the agglomerates larger than 200 nm may be aligned to the electric field in the DMA.

Table 3 shows deviation of measured surface area from different methods with respect to APM–TEM method for various diameters for all aerosol types used in this study.

To probe the measurement error introduced by different instruments for different aerosols, calculations were performed to compare surface area of true fractal agglomerates (of spherical primary particles) obtained from measured sensitivity  $\sigma$  (see Section 3.4 for details) of each instrument with actual surface area obtained using fractal theory and the approach outlined by Sorensen (2011). A lognormal distribution of mobility diameters was assumed for the polydisperse aerosol with known total number concentration ( $N_{tot}$ ), geometric mean mobility diameter ( $d_{gm}$ ), and geometric standard deviation ( $\sigma_g$ ). Further, it was assumed that each agglomerate particle was a true fractal with primary particle size  $d_p$  with total of  $N_p$  primary particles. The mobility diameter of the fractal aggregate was computed using the approach outlined by Sorensen (2011; Eq. (25)). Then, a number of primary particles,  $N_p$ , for each agglomerate mobility diameter  $d_{mob}$  was calculated. The estimated total surface area,  $S_{est}$ , of the aerosol distribution was obtained by summation of  $N_p \pi d_p^2 dN$  in each size bin (that is,

$\int_0^\infty (N_{tot} / \sqrt{2\pi} d_{mob} \ln \sigma_g) \exp(-((\ln d_{mob} - \ln d_{gm})^2 / 2(\ln \sigma_g)^2)) N_p \pi d_p^2 dd_{mob}$ ). The surface area of the polydisperse aerosol that would be obtained from each instrument was calculated using the measured sensitivity  $\sigma$  of each instrument shown in Fig. 6. The comparison of true total surface area ( $S_{est}$ ; from fractal theory) and that from all experimental approaches used in this work is shown in Table 4. Surface area of polydisperse aerosols is underestimated by all diffusion charging approaches. For aerosols with mean geometric diameter larger than about 600 nm, the surface area can be underestimated by the diffusion chargers by up to an order of magnitude.

### 3.4. Measurement sensitivity

Fig. 6a and b shows sensitivity for each instrument as a function of mobility diameter for silver and TiO<sub>2</sub> agglomerates, respectively. The sensitivity  $\sigma$  is defined as a ratio of surface area measured by each of the instruments to surface area from APM–TEM.  $\sigma=1$  represents the sensitivity of the APM–TEM approach.

Fig. 6a and b shows that for silver agglomerates having open structure ( $D_f=2.0$ ), the sensitivities of LQ1-DC and DC2000CE decrease with increasing mobility diameter by a factor of 2 or 3 while the sensitivity of mobility-diameter approach (MD) is relatively constant. The sensitivity of NSAM seems to fluctuate. On the other hand, for TiO<sub>2</sub> agglomerates having very compact structure ( $D_f=2.634$ ), both sensitivities of MD and DC2000CE decrease with increasing mobility diameter.

Fig. 7 shows sensitivity ( $\sigma$ ) as a function of mass scaling factor ( $D_f$ ) for all the aerosols studied in this work. The particle structure or morphology has a pronounced effect on the mobility-based method compared to DCS methods. As particle structure becomes more compact, i.e., as mass scaling factor increases, sensitivity of the MD methods decreases.

## 4. Conclusions

Four different approaches for measuring surface area of submicrometer particles were compared in this study: (i) diffusion charging-based sensors (three sensors from three manufacturers were evaluated: TSI Inc., model 3550 nanoparticle surface area monitor; Ecochem, model DC2000CE diffusion charger; Matter Engineering, model LQ1-DC diffusion charger), (ii) mobility diameter-based surface area estimation, (iii) surface area based on mobility diameter assuming a linear chain morphology of an agglomerate with uniform primary particle size (MD-LCA), and finally, (iv) the surface area estimation based on the mass measurement from APM and primary particle size measurement using TEM (APM-TEM). It was shown that the APM-TEM method, which can be applied directly to airborne particles unlike the BET method, agrees well with the BET method. It was also found that the response of the three diffusion charging-based sensors to silver agglomerates substantially underestimated the surface area measured by the APM-TEM approach by a factor of 3–10 in the size range studied. These differences in surface area measured by diffusion charging-based sensors could be more drastic for large complex aerosols with high dynamic shape factors and large internal area. Mobility diameter-based methods (MD and MD-LCA) generally gave good agreement at low mobility sizes; however, they significantly underestimated surface area at large mobility diameters. MD and MD-LCA approaches were sensitive to the structure or morphology of the particles. Measurements for particles with open structure with  $D_f < 2$  were reliable using the MD and MD-LCA approaches. The results show that caution should be exercised in the interpretation of measurements from diffusion charging-based instruments. Also the mobility diameter-based surface area measurements may be relatively reasonable for open agglomerates with no internal surface area, but may significantly underestimate surface area of compact agglomerates.

## Acknowledgments

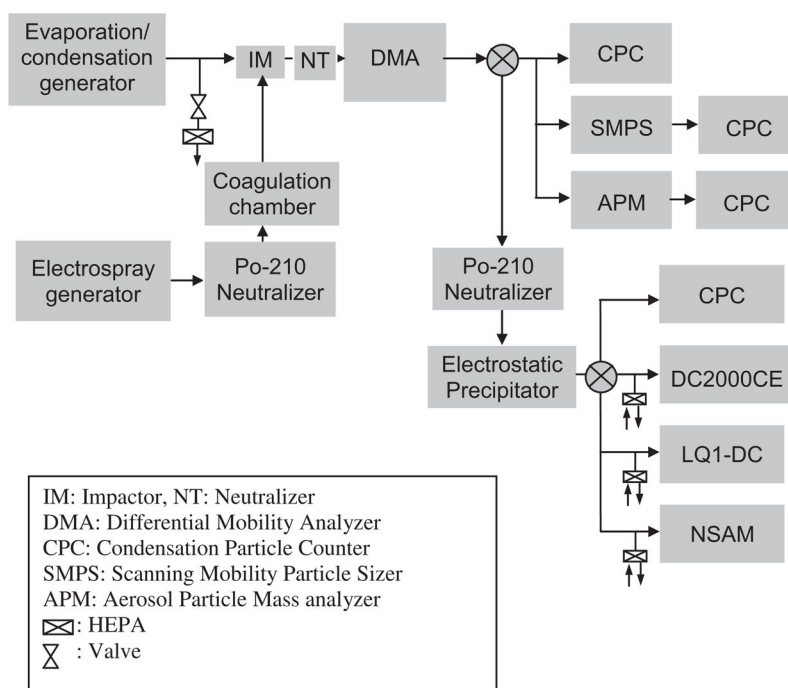
The authors would like to thank Drs. Art Miller and Emanuele Cauda at NIOSH for helpful suggestions, and Ellen Galloway for editorial assistance. This work was funded by the National Institute for Occupational Safety and Health through the Nanotechnology Research Center program (Project CAN 927ZBCL).

## References

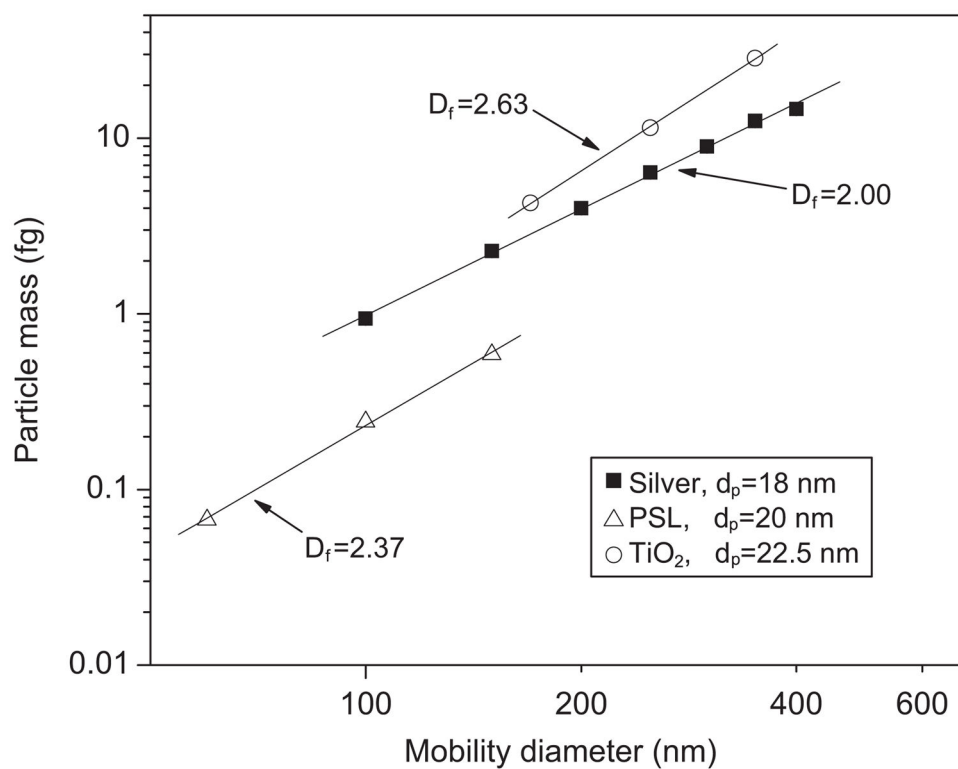
- Barone TL, Lall AA, Storey JME, Mulholland GW, Prikhodko VY, Frankland JH, et al. Size-resolved density measurements of particle emissions from an advanced combustion diesel engine: effect of aggregate morphology. *Energy Fuels*. 2011; 2011(25):1978–1988.
- Bau S, Witschger O, Gensdarmes F, Thomas D. Response of three instruments devoted to surface-area for monodisperse and polydisperse aerosols in molecular and transition regimes. *Journal of Physics*. 2011; 304:012015.
- Braydich-Stolle LK, Schaeublin NM, Murdock RC, Jiang J, Biswas P, Schlager JJ, et al. Crystal structure mediates mode of cell death in TiO<sub>2</sub> nanotoxicity. *Journal of Nanoparticle Research*. 2009; 11(6):1361–1374.
- Brouwer D, van Duuren-Stuurman B, Berges M, Jankowska E, Bard D, Mark D. From workplace air measurement results toward estimates of exposure? Development of a strategy to assess exposure to manufactured nano-objects. *Journal of Nanoparticle Research*. 2009; 11:1867–1881.
- Buonanno G, Morawska L, Stabile L, Viola A. Exposure to particle number, surface area and PM concentrations in pizzerias. *Atmospheric Environment*. 2010; 44:3963–3969.
- Chan P, Dahneke B. Free-molecular drag on straight chains of uniform spheres. *Journal of Applied Physics*. 1981; 52:3106–3110.

- Dhaniyala, S.; Fierz, M.; Keskinen, J.; Mariamaki, M. Instruments based on electrical detection of aerosols. In: Kulkarni, P.; Baron, PA.; Willeke, K., editors. *Aerosol Measurement: Principles, Techniques, and Applications*. John Wiley and Sons; New York: 2011.
- Ehara K, Hagwood C, Coakley KJ. Novel method to classify aerosol particles according to their mass-to-charge ratio-aerosol particle mass analyzer. *Journal of Aerosol Science*. 1996; 27:217–234.
- Elihn K, Berg P. Ultrafine particle characteristics in seven industrial plants. *Annals of Occupational Hygiene*. 2009; 53(5):475–484.
- Evans DE, Ku BK, Birch ME, Dunn KH. Aerosol monitoring during carbon nanofiber production: mobile direct-reading sampling. *Annals of Occupational Hygiene*. 2010; 52:9–21.
- Fissan H, Neumann S, Trampe A, Pui DYH, Shin WG. Rationale and principle of an instrument measuring lung deposited nanoparticle surface area. *Journal of Nanoparticle Research*. 2007; 9:53–59.
- Gäggeler HW, Baltensperger U, Emmenegger M, Jost DT, Schmidt-Ott A, Haller P, Hofmann M. The epiphaniometer, a new device for continuous aerosol monitoring. *Journal of Aerosol Science*. 1989; 20:557–564.
- Hinds, WC. *Aerosol Technology*. 2. Wiley; New York: 1999.
- ICRP (International Commission on Radiological Protection), W.C. *Human Respiratory Tract Model for Radiological Protection*. Oxford: Pergamon Press, Elsevier Science Ltd; 1994. ICRP Publication 66
- Keller A, Fierz M, Siegmann K, Siegmann HC, Filippov A. Surface science with nanosized particles in a carrier gas. *Journal of Vacuum Science and Technology A*. 2001; 19:1–8.
- Kim SC, Wang J, Emery MS, Shin WG, Mulholland GW, Pui DYH. Structural property effect of nanoparticle agglomerates on particle penetration through fibrous filter. *Aerosol Science and Technology*. 2009; 43(4):344–355.
- Ku, BK. Diffusion charger-based aerosol surface-area monitor response to airborne spherical particles 100–800 nm in diameter. *Proceedings of the Abstracts of the 4th International Conference on Nanotechnology—Occupational and Environmental Health; August 25–29; Helsinki, Finland*. 2009. p. 46
- Ku BK. Determination of the ratio of diffusion charging-based surface area to geometric surface area for spherical particles in the size range of 100–900 nm. *Journal of Aerosol Science*. 2010; 41(9): 835–847.
- Ku BK, Kulkarni P. Morphology of single-wall carbon nanotube aggregates generated by electrospray of aqueous suspensions. *Journal of Nanoparticle Research*. 2009; 11:1393–1403.
- Ku BK, Maynard AD. Comparing aerosol surface-area measurement of monodisperse ultrafine silver agglomerates using mobility analysis, transmission electron microscopy and diffusion charging. *Journal of Aerosol Science*. 2005; 36:1108–1124.
- Ku BK, Maynard AD. Generation and investigation of airborne silver nanoparticles with specific size and morphology by homogeneous nucleation, coagulation and sintering. *Journal of Aerosol Science*. 2006; 37:452–470.
- Ku BK, Emery MS, Maynard AD, Stolzenburg M, McMurry PH. In situ structure characterization of airborne carbon nanofibers by a tandem mobility–mass analysis. *Nanotechnology*. 2006; 17:3613–3621. [PubMed: 19661613]
- Lall AA, Friedlander SK. On-line measurement of ultrafine aggregate surface area and volume distributions by electrical mobility analysis: I. Theoretical analysis. *Journal of Aerosol Science*. 2006; 37:260–271.
- Lall AA, Seipenbusch M, Rong WZ, Friedlander SK. On-line measurement of ultrafine aggregate surface area and volume distributions by electrical mobility analysis: II. Comparison of measurements and theory. *Journal of Aerosol Science*. 2006; 37:272–282.
- LeBlanc A, Moseley A, Chen B, Frazer D, Castranova V, Nurkiewicz T. Nanoparticle inhalation impairs coronary microvascular reactivity via a local reactive oxygen species-dependent mechanism. *Cardiovascular Toxicology*. 2010; 10(1):27–36. [PubMed: 2003351]
- LeBouf RF, Ku BK, Chen BT, Frazer DG, Cumpston JL, Stefaniak AB. Measuring surface area of airborne titanium dioxide powder agglomerates: relationships between gas adsorption, diffusion and mobility-based methods. *Journal of Nanoparticle Research*. 2011; 13(12):7029–7039.

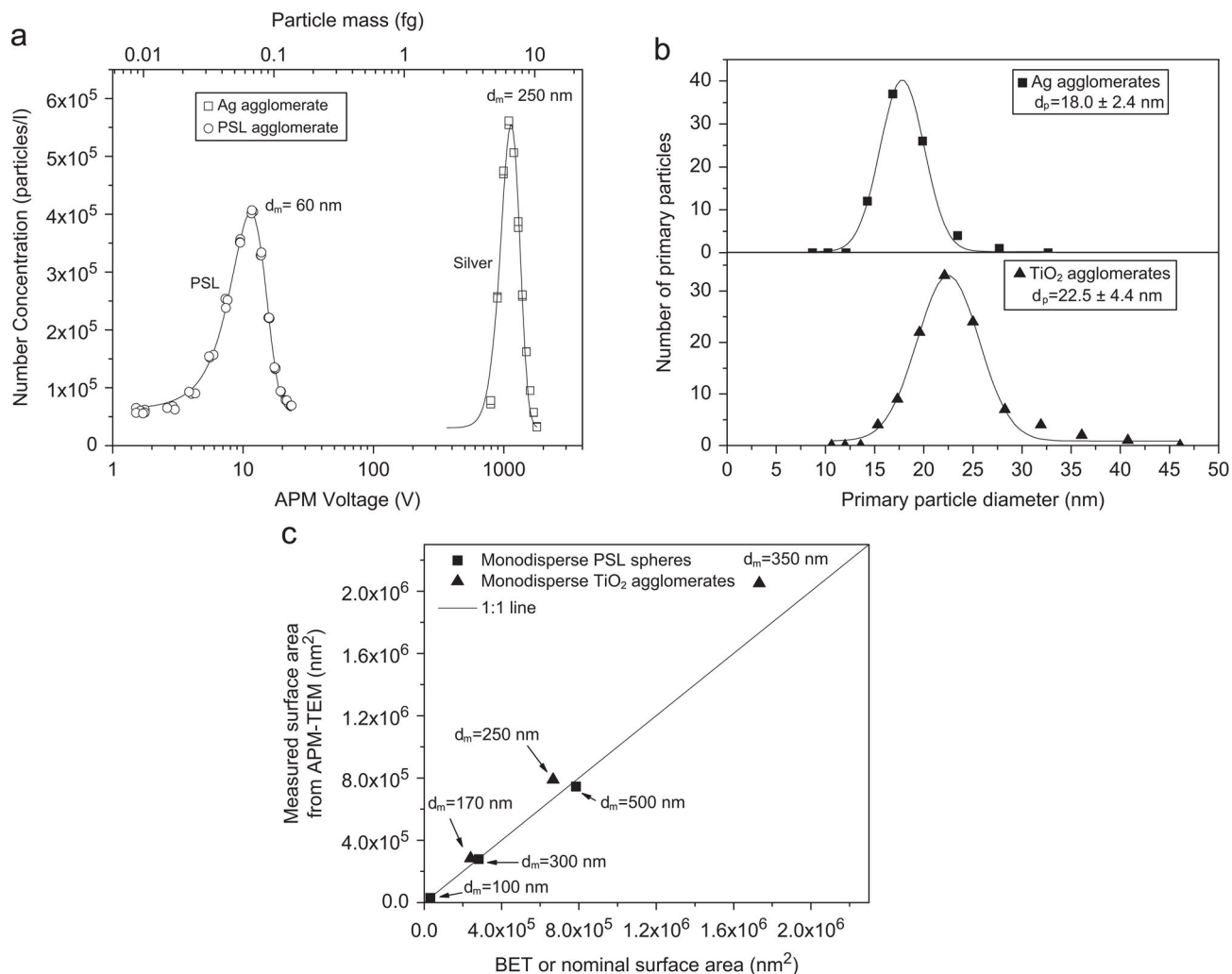
- Matter Engineering AG. Operating Manual of LQ1-DC. 2001.
- Nel A, Xia T, Mädler L, Li N. Toxic potential of materials at the nanolevel. *Science*. 2006; 311:622–627. [PubMed: 16456071]
- Ntziachristos L, Polidori A, Phuleria H, Geller MD, Sioutas C. Application of a diffusion charger for the measurement of particle surface concentration in different environments. *Aerosol Science and Technology*. 2007; 41:571–580.
- Nurkiewicz T, Porter D, Hubbs A, Stone S, Chen B, Frazer D, Boegehold M, Castranova V. Pulmonary nanoparticle exposure disrupts systemic microvascular nitric oxide signaling. *Journal of Toxicological Science*. 2009; 110(1):191–203.
- Oberdörster G, Maynard A, Donaldson K, Castranova V, Fitzpatrick J, Ausman K, et al. Principles for characterizing the potential human health effects from exposure to nanomaterials: elements of a screening strategy. *Particle and Fibre Toxicology*. 2005; 2(8)10.1186/1743-8977-2-8
- Park JY, Raynor PC, Maynard AD, Eberly LE, Ramachandran G. Comparison of two estimation methods for surface area concentration using number concentration and mass concentration of combustion-related ultrafine particles. *Atmospheric Environment*. 2009; 43:502–509.
- Sager TM, Castranova V. Surface area of particle administered versus mass in determining the pulmonary toxicity of ultrafine and fine carbon black: comparison to ultrafine titanium dioxide. *Particle and Fibre Toxicology*. 2009; 6(15)10.1186/1743-8977-6-15
- Singh S, Shi T, Duffin R, Albrecht C, van Berlo D, Hohr D, Fubini B, Martra G, Fenoglio I, Borm PJA, Schins RPF. Endocytosis, oxidative stress and IL-8 expression in human lung epithelial cells upon treatment with fine and ultrafine TiO<sub>2</sub>: Role of the specific surface area and of surface methylation of the particles. *Toxicology and Applied Pharmacology*. 2007; 222:141–151. [PubMed: 17599375]
- Sorensen CM. The mobility of fractal aggregates: a review. *Aerosol Science and Technology*. 2011; 45(7):765–779.
- Stoeger T, Reinhard C, Takenaka S, Schroepfel A, Karg E, Ritter B, Heyder J, Schulz H. Instillation of six different ultrafine carbon particles indicates a surface area threshold dose for acute lung inflammation in mice. *Environmental Health Perspectives*. 2006; 114:328–333. [PubMed: 16507453]
- Suttiponparnit K, Jiang J, Sahu M, Suvachittanont S, Charinpanitkul T, Biswas P. Role of surface area, primary particle size, and crystal phase on titanium dioxide nanoparticle dispersion properties. *Nanoscale Research Letters*. 2011; 6:27.

**Fig. 1.**

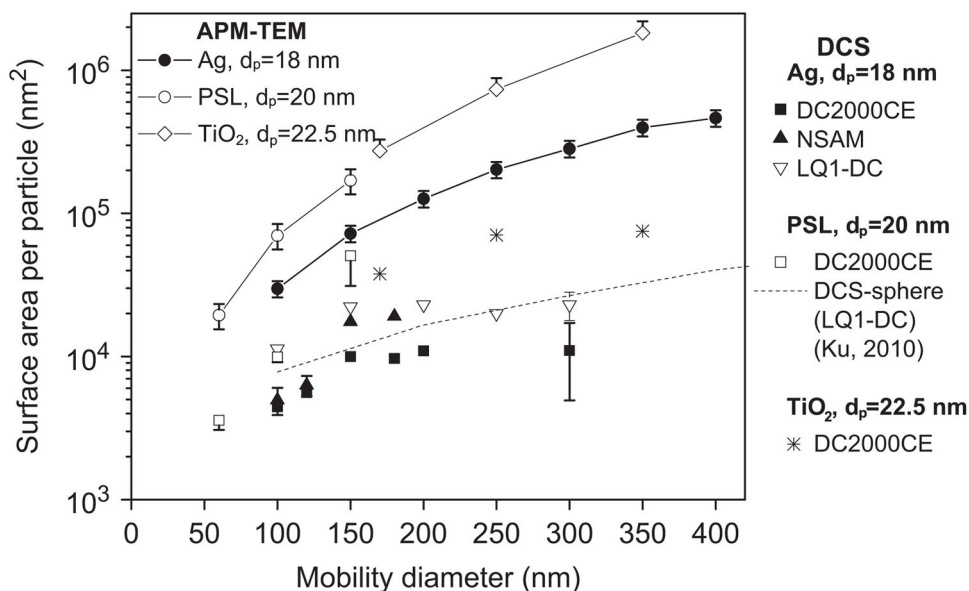
Experimental setup. Evaporation/condensation generator was used to produce silver agglomerates, and electro spray generator used to generate polystyrene latex particles. DC2000CE (Ecochem), LQ1-DC (Matter Engineering), and NSAM (TSI Inc.) are diffusion charging-based instruments.



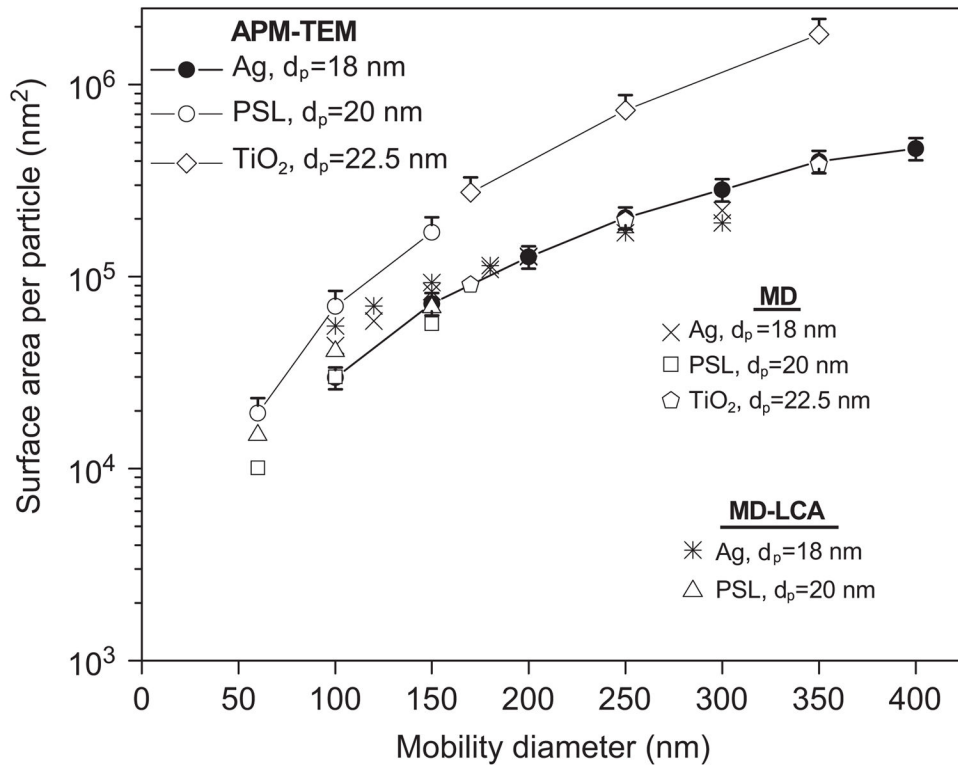
**Fig. 2.** Log-log plot of mass versus mobility diameter for three different agglomerates: silver agglomerate ( $d_p=18$  nm), PSL agglomerate ( $d_p=20$  nm), and TiO<sub>2</sub> agglomerate ( $d_p=22.5$  nm). The mass scaling factor,  $D_f$ , is equal to the slope of the linear fit.

**Fig. 3.**

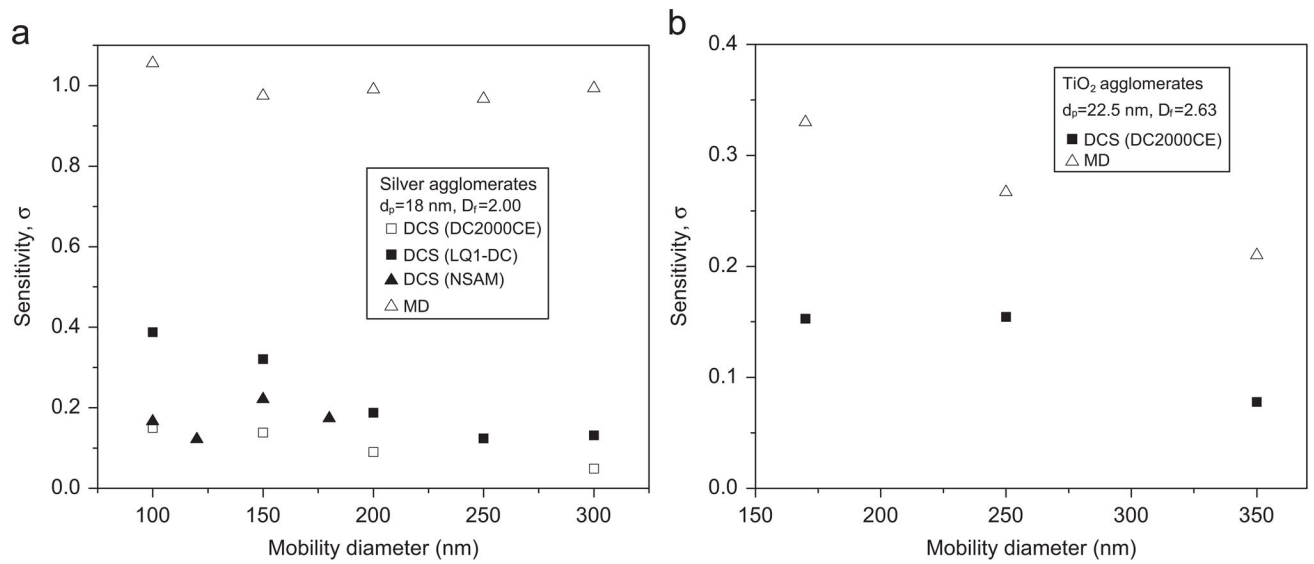
(a) Number distributions measured downstream of the APM as a function of the APM classifying voltage for mobility-selected aerosol particles of silver and PSL. The peak voltage was used to determine the “average” particle mass of DMA-classified agglomerate particles. Top x-axis represents particle mass assuming one charge per particle. (b) Primary particle size distribution measured by TEM for silver and  $TiO_2$  agglomerates. (c) Comparison of surface area from mass measured by APM–TEM with input surface area calculated on the basis of nominal mobility diameter classified by DMA for spherical PSL particles. Nominal surface area for PSL spheres is calculated from PSL spherical diameter, and for  $TiO_2$  is calculated from multiplying BET-measured specific surface area of bulk  $TiO_2$  material by particle mass measured by APM.



**Fig. 4.** Comparison of diffusion charging-based surface area (DCS) with the APM-TEM method for three different particle agglomerates. Normalized surface area on y-axis is surface area per particle. Error bars for the APM-TEM measurements correspond to the uncertainty from the variation of primary particle sizes within one standard deviation or 20%.



**Fig. 5.** Comparison of mobility-based surface area (MD and MD-LCA) with the APM-TEM method for three different particle agglomerates.

**Fig. 6.**

(a) Sensitivity for each instrument as a function of mobility diameter for silver agglomerates with primary particle diameter of 18 nm. The sensitivity  $\sigma$  is defined as a ratio of surface area measured by each of the instruments to surface area from APM-TEM. (b) Sensitivity for each instrument as a function of mobility diameter for  $\text{TiO}_2$  agglomerates with primary particle diameter of 22.5 nm. The sensitivity  $\sigma$  is defined as a ratio of surface area measured by each of the instruments to surface area from APM-TEM.

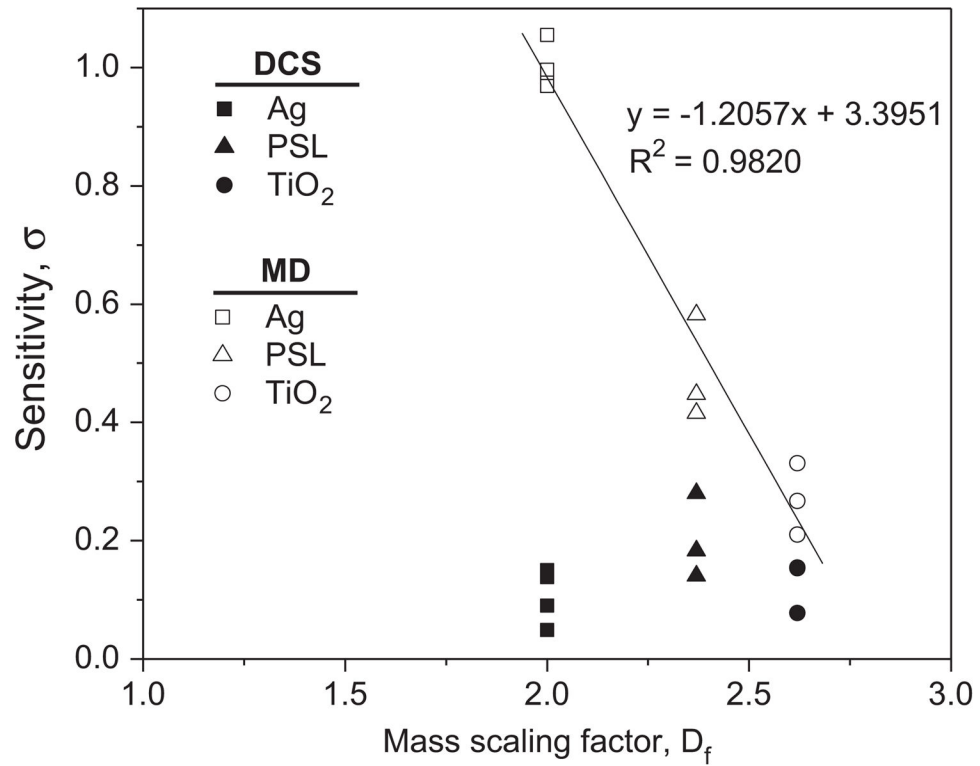


**Fig. 7.** Sensitivity ( $\sigma$ ) for DC-based sensor and mobility diameter-based approach as a function of particle structure.  $D_f$  represents fractal dimension-like mass scaling factor.

**Table 1**

Definition of different surface area from each instrument.

<b>Instrument</b>	<b>Definition</b>
LQ1-DC, DC2000CE	Active surface area is defined as the surface of a particle that is involved in interactions with the surrounding gas Keller et al. (2001)
NSAM	Lung-deposited surface area is defined as the surface of a particle deposited in the alveolar or tracheobronchial region with its deposition efficiency based on the ICRP curve Fissan et al. (2007)
SMPS	Mobility diameter-based surface area assuming spherical particles
APM-TEM	Surface area assuming all primary particles have the same size, and no necking between primary particles
BET	Surface area based on nitrogen adsorption and analysis of the data using the Brunauer-Emmet-Teller isotherm

**Table 2**Surface area calculation of TiO<sub>2</sub> particles from BET measurements.

$d_m$ (nm)	$m_p$ from APM (fg)	SSA from BET (m <sup>2</sup> /g)	SA ( $m_p \times$ SSA) (nm <sup>2</sup> )
170	4.052	59.3	240283.6
250	11.25	59.3	667125
350	29.23	59.3	1733339

Author Manuscript

Author Manuscript

Author Manuscript

Author Manuscript

**Table 3**

Surface area difference of each approach relative to surface area ( $S_{\text{APM-TEM}}$ ) measured by APM-TEM method for silver agglomerates ( $d_p = 18$  nm), PSL agglomerates ( $d_p = 20$  nm), and  $\text{TiO}_2$  agglomerates ( $d_p = 22.5$  nm). Surface area difference (%) was calculated based on  $(S_{\text{APM-TEM}} - S)/S_{\text{APM-TEM}} \times 100$ .

Mobility diameter (nm)	DC2000CE	LQ1-DC	NSAM	MD <sup>a</sup>	MD-LCA <sup>b</sup>
<i>Silver</i>					
100	85.03	62.03	83.30	-47.07	-86.02
120	-	-	86.55	-	-
150	86.20	69.28	73.17	-15.54	-28.37
180	-	-	81.84	-	-
200	91.37	81.86	-	-0.06	-0.85
250	-	90.12	-	7.76	16.64
300	96.12	91.89	-	22.14	33.06
<i>PSL</i>					
60	81.55	-	-	41.80	22.81
100	85.84	-	-	55.20	41.68
150	70.30	-	-	58.40	59.33
<i>TiO<sub>2</sub></i>					
170	86.23	-	-	66.94	-
250	90.38	-	-	73.31	-
350	97.04	-	-	78.99	-

<sup>a</sup> MD=mobility diameter

<sup>b</sup> MD-LCA=mobility diameter and linear chain approximation

Comparison of total surface area of a polydisperse aerosol (with each particle being an agglomerate) obtained from fractal theory to that predicted for mobility diameter and diffusion charging sensor approaches using measured sensitivity  $\sigma$  for each instrument.

**Table 4**

$d_g$ (nm)	$S_{est}^a$ ( $\mu\text{m}^2/\text{cm}^3$ )	S_MD	S_DCS (DC2000CE)	S_DCS (LQ1-DC)	S_DCS (NSAM)
<i>Ag, 18 nm</i>					
50	2.59E+02	2.67E+02	3.63E+01	8.81E+01	4.15E+01
100	1.25E+03	1.29E+03	1.76E+02	4.26E+02	2.01E+02
200	4.65E+03	4.79E+03	6.50E+02	1.58E+03	7.43E+02
300	1.16E+04	1.19E+04	1.62E+03	3.93E+03	1.85E+03
400	2.70E+04	2.78E+04	3.78E+03	9.17E+03	4.32E+03
600	7.15E+04	7.36E+04	1.00E+04	2.43E+04	-
800	1.46E+05	1.50E+05	2.04E+04	4.95E+04	-
1000	2.54E+05	2.62E+05	3.56E+04	8.65E+04	-
2000	1.60E+06	1.65E+06	2.24E+05	5.45E+05	-
$d_g$ (nm)	$S_{est}$ ( $\mu\text{m}^2/\text{cm}^3$ )	S_MD	S_DCS (DC2000CE)	S_DCS (LQ1-DC)	S_DCS (NSAM)
<i>TiO<sub>2</sub>, 22.5 nm</i>					
100	1.96E+03	4.90E+02	2.16E+02	-	-
400	4.21E+04	1.05E+04	4.64E+03	-	-
600	1.12E+05	2.79E+04	1.23E+04	-	-
800	2.27E+05	5.69E+04	2.50E+04	-	-
1000	3.97E+05	9.94E+04	4.37E+04	-	-
2000	2.50E+06	6.26E+05	2.75E+05	-	-

<sup>a</sup> Calculated using a relation between mobility diameter and number of primary particles in an agglomerate based on the fractal theory work of Sorensen (2011). Total number concentration ( $N_{tot}$ ) is 10,000  $\text{cm}^{-3}$  and geometric standard deviation ( $\sigma_g$ ) is 2.0 assumed.